Expression and Molecular Regulation of the *Cox2* Gene in Gastroenteropancreatic Neuroendocrine Tumors and Antiproliferation of Nonsteroidal Anti-Inflammatory Drugs (NSAIDs)

Authors' Contribution:
Study Design A
Data Collection B
Statistical Analysis C
Data Interpretation D
Manuscript Preparation E
Literature Search F
Funds Collection G

BCD 1 **Feng Gao**
EF 1 **Mohammad Ishraq Zafar**
AD 2,3 **Stefan Jüttner**
AB 2,4 **Michael Höcker**
AG 2 **Bertram Wiedenmann**

1 Department of Endocrinology, Union Hospital, Tongji Medical College, Huazhong University of Science and Technology, Wuhan, P.R. China
2 Medical Department, Division of Hepatology and Gastroenterology (including Metabolic Diseases), Charité, Campus Mitte (CCM) and Campus Virchow-Klinikum (CVK), Berlin, Germany
3 Department of Pathology, Pathologie Ansbach, Ansbach, Germany
4 HMNC Holding, München, Germany

Corresponding Author: Feng Gao, e-mail: gaofengwh@aliyun.com
Source of support: The current work was supported by German DFG-Graduiertenkollegs 276/3 "Signal recognition and transduction"

Background: Gastroenteropancreatic neuroendocrine tumors (GEP-NETs) has had a significant increase over the past 4 decades. The pathophysiological role of the *cyclooxygenase-2* (*cox-2*) gene and factors responsible for the expression in GEP-NETs is of clinical value. Current study determined the expression of *cox-2* gene in human GEP-NET tissues and corresponding cell lines, investigated the molecular mechanisms underlying the regulation of *cox-2 gene* expression and assessed the effect of nonsteroidal anti-inflammatory drugs (NSAIDs) on both anchorage-dependent and independent growth of GEP-NET cells.

Material/Methods: GEP-NET tissues and QGP-1, BON, and LCC-18 GEP-NET cell lines were used. The expression of *cox-2* gene was analyzed by immunohistochemistry, western blot, RT-PCR, and enzyme immunoassay. Transient transfection and luciferase assays along with electrophoretic mobility shift assays were conducted to explore the regulation of *cox-2* gene expression. The effect of COX-inhibitors on GEP-NET cell growth was determined by proliferation assays and colony growth assessment.

Results: We found 87.8% of GEP-NET tissues stained positive for COX-2. QGP-1 and LCC-18 cells expressed *cox-2* gene. PGE2 (prostaglandin E2) amounts quantified in the supernatants of NET cells matched to *cox-2* expression level. The CRE-E-box element (–56 to –48 bp) and binding of USF1, USF2, and CREB transcription factors to this proximal promoter element were essential for *cox-2* promoter activity in GEP-NET cells. COX-2-specific inhibitor NS-398 potently and dose-dependently inhibited PGE2 release from QGP-1 cells. Interestingly, both NS-398 and acetylic salicylic acid effectively suppressed proliferation of QGP-1 and BON cells in a dose-dependent manner.

Conclusions: The majority of GEP-NETs over express *cox-2* gene. The binding of CREB and USF-1/-2 transcription factors to a proximal, overlapping CRE-Ebox element is the underlying mechanism for *cox-2 gene* expression. NSAIDs potently suppressed the proliferations and may offer a novel approach for chemoprevention and therapy of GEP-NETs.

MeSH Keywords: Anti-Inflammatory Agents, Non-Steroidal • Cyclooxygenase 2 Inhibitors • Neuroendocrine Tumors

Full-text PDF: https://www.medscimonit.com/abstract/index/idArt/912419
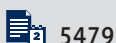
📄 5479   📊 2   📈 9   📚 43

Background

Neuroendocrine tumors (NETs) have biological pathways connected to the endocrine cells of the diffuse endocrine system (DES). This leads to the potential for different primary localizations of these tumors [1]. DES cells are mainly found in the digestive system, and to a lesser extent in the respiratory system. Reduced amounts are also present in other locations, including the urogenital tract, skin (Merkel cells), and thyroid gland (calcitonin-producing cells) [2]. The components of the DES share antigens with nerve elements and are therefore classified as neuroendocrine [3].

A specific type of NETs known as gastroenteropancreatic neuroendocrine tumors (GEP-NETs) has significantly increased over the past 4 decades, GEP-NETs account for approximately 1.5% of all gastrointestinal and pancreatic neoplasms and are currently estimated to occur in 3.0 to 5.2 cases per 100 000 persons every year [4]. In general, GEP-NETs exhibit low proliferating activity. For patients with low and moderately differentiated metastases, the 5-year survival probability is 35%, whereas, in patients with poorly differentiated distant metastases, it is only 4% [5].

No risk factors have been identified, but women of African-American, Hispanic, and Asian descent are more predisposed to GEP-NETs. Also, the risk is higher when a person has certain medical conditions, including hypergastrinemia, preexisting diabetes mellitus, and ulcerative colitis [4]. Up to 25% of GEP-NETs occur alongside complex genetic syndromes, including MEN-1 (Wermer syndrome), neurofibromatosis type 1 (NF-1 or von Recklinghausen disease), von-Hippel-Lindau disease, and tuberous sclerosis complex [4].

GEP-NETs are classified into carcinoids and pancreatic endocrine tumors [6]. Some GEP-NET cells called functioning NETs can produce neuropeptides, resulting in clinical symptoms. GEP-NETs are characterized by expression of differentiation markers of neuroendocrine origin [7]. These markers include chromogranin A (CgA), synaptophysin (small synaptic vesicles, SSV), neuron-specific enolase, and 2 isoforms of ATP-dependent vesicular monoamine transporter protein (VMAT1 and VMAT2) [8].

Except in tumors in patients with specific genomic gene alterations, such as MEN-1 syndrome and von Hippel Lindau disease, molecular events determining the uncontrolled growth of neuroendocrine cells are still unclear. The *cyclooxygenase-2* (*cox-2*) gene has been linked to tumorigenesis in both premalignant tissues and malignant tumors [9]. Additional evidence supporting a cause-effect relationship between overexpression of *cox-2* gene and carcinogenesis has been found [10]. Oshima and colleagues [11] assessed the development of intestinal adenomas in wild-type and homozygous *cox-2* null

Apc$^{\Delta 716}$ knockout mice (a model of human familial adenomatous polyposis, in which a targeted truncation deletion in the tumor suppresser gene *APC* causes intestinal adenomatous polyposis). The number and size of polyps decreased by 86% in the *cox-2* null mice compared with *cox-2* wild-type mice, but the loss of one allele of the *cox-2* gene led to a 66% decrease in the number of polyps.

Inhibitors such as celecoxib and rofecoxib, which specifically target the *cox-2* gene, prevent intestinal, breast, skin, lung, bladder, and tongue tumors from forming in rodents [12]. The selective COX-2 inhibitors also suppress the growth of established tumors, including skin epidermal, head and neck, colorectal, stomach, esophageal, pancreatic, gallbladder, lung, breast, and prostate tumors [12].

Whether nonsteroidal anti-inflammatory drugs (NSAIDs) suppress tumor progression only by blocking prostaglandin synthesis is under considerable debate. Several studies indicate that COX-independent pathways (e.g., PPARδ pathway) are also critical in the cancer chemopreventive properties of NSAIDs [13–15]. Therefore, both COX-dependent and COX-independent pathways may be involved in the anticancer properties of NSAIDs.

The current study determines the expression of *cox-2* gene in human GEP-NET tissues and corresponding cell lines and investigates the underlying molecular mechanisms regulating this gene expression; we identified the promoter elements and transcription factors mediating basal *cox-2* expression in GEP-NET cells. The effects of 2 NSAIDs on anchorage-dependent cell proliferation were also analyzed in the COX-2-positive QGP-1 cell line.

Material and Methods

The growth of cell lines and cell culture

Three human GEP-NET cell lines: QGP-1 [16,17], BON [18,19], and LCC-18 [20,21]; and a *cox-2* overexpressing gastric carcinoma cell line MKN-45 [22,23] were used in this study (Table 1). QGP-1 cells were grown in RPMI 1640 medium (Gibco Life Sciences, Karlsruhe, Germany) and the other 3 were grown in Dulbecco's Modified Eagle Medium (DMEM, Gibco) in a humidified 5% CO_2 incubator at 37°C. All culture media were supplemented with 4 mM glutamine (Biochrom KG, Berlin, Germany), 100 U/mL penicillin, 100 μg/mL streptomycin (Biochrom KG, Berlin, Germany), and 10% fetal calf serum (FCS, Gibco).

Selection of tumor tissue specimens

All specimens were surgical resection specimens obtained from the Department of Hepatology and Gastroenterology, Charité

Table 1. Cell lines.

Name	Description	Reference
QGP-1	Human nonfunctioning pancreatic islet cell carcinoma poorly differentiated	[16,17]
BON	Human functioning pancreatic carcinoid well differentiated	[18,19]
LCC-18	Human neuroendocrine colonic carcinoma poorly differentiated	[20,21]
MKN-45	Human gastric carcinoma poorly differentiated isolation from liver metastasis	[22,23]

Table 2. Alkaline phosphatase/anti-alkaline phosphatase (APAAP) procedure.

Methods	Procedures
Deparaffining of tissue and rehydration	Tumor sample sections were deparaffinized with Rotihistol, followed by washes in decreasing concentrations of alcohol, after which they were incubated in citrate buffer (10 mM sodium citrate, pH 6)
Unmasking of antigens	Sections were treated in a pressure-cooking pot for 2 minutes (repeated 3 times). The buffer was replaced between treatments. Sections were washed in Tris-buffered saline (TBS)
Addition of primary and secondary antibodies	Sections were incubated with a primary mouse monoclonal antibody against human COX-2 at a dilution of 1: 1000 overnight at 4°C. Sections were washed with TBS. The secondary rabbit antimouse streptavidin-coated polyclonal antibody was added at a dilution of 1: 50
APAAP complex	APAAP complex was also added at a dilution of 1: 50 and sections were washed
Counterstaining and covering	Counterstaining with Mayer's hematoxylin solution was performed for 4 minutes at room temperature. Slides were washed with tap water and covered with glycerol gelatin

– Universitätsmedizin Berlin. Tissue specimens were frozen in liquid nitrogen immediately after surgical removal. All tissues had histologically proven GEP-NETs. The current study was approved by the institutional ethical committee of the Charité – Universitätsmedizin, Germany.

Immunohistochemistry

In this study, the alkaline phosphatase/anti-alkaline phosphatase (APAAP) method was used (Table 2). APAAP is a type of immunohistochemical staining technique used to label specific antigens with monoclonal or polyclonal antibodies [24]. A compound called APAAP complex was used in conjunction with a primary and secondary antibody, resulting in an intense signal without endogenous interference [25].

RNA extraction and RT-PCR

RNA extraction was done in cell lines and tumor tissues. RNA was extracted with TRIzol® reagent (Gibco Life Sciences, Karlsruhe, Germany) and suspended in DEPC-treated water. Absorbance was determined at a wavelength of 260 nm and 280 nm. Only RNA with a 260/280 ratio of >1.6 was used.

A 2-step RT (reverse transcription) and *gapdh*-controlled duplex PCR for human *cox-1* or *cox-2* were performed. After 30 cycles

of PCR, 15 µL of each product plus 5 µL of DNA-sample buffer was loaded on 2% agarose gels. Samples were electrophoresed at 100V in TAE running buffer, and the results were made visible under UV light

Western blot analysis

After the GEP-NET cells were cultured overnight, the medium was replaced by fresh serum-free Ultraculture® medium for 24 hours. The cells were then lysed with 200 µL of Buffer C and Nonidet P-40 (Boehringer, Mannheim). Then 100 mg to 200 mg of tumor tissue was homogenized in 1 mL of 50 mM Tris pH 7.0, 0.15 M NaCl, 0.1% NaN_3, 0.1% NP-40, 2 mM PMSF, 2 mM benzamidine, 2 µg/mL aprotinin, and 20 µg/mL leupeptin. A 500-µL detergent mix consisting of 50 mM Tris pH 7.0, 0.15 M NaCl, 0.1% NaN_3, 3% NP-40, and 1.5% sodium deoxycholate was added. After 20 minutes of incubation at 4°C, the cell debris or tumor tissue lysates were centrifuged at 12 000*g* for 10 minutes at 4°C.

Electrophoresis with NuPAGE® Bis-Tris system (Invitrogen, Karlsruhe) was conducted, and gels were blotted onto nitrocellulose membranes (Hybond ECL, Amersham Pharmacia Biotech, Braunschweig, Germany) with electrophoresis. To stain the proteins and ensure that equal amounts of protein were loaded in each compartment, the membranes were immersed in 0.5%

Ponceau S (Sigma Chemical Co., St. Louis, MO, USA) in 1% acetic acid, and incubated in blocking solution (TBST plus 5% nonfat dried milk) at room temperature for 2 hours to block nonspecific binding. The samples were incubated with the primary antibody mouse antihuman COX-1 (1: 1000 dilution, Cayman Chemicals, Ann Arbor, MI, USA) or mouse antihuman COX-2 (1: 4000 dilution, Cayman Chemicals, Ann Arbor, MI, USA) in blocking solution on a shaker overnight at 4°C.

After extensive washing in TBST, proteins were detected with an enhanced chemical luminescence (ECL) method. Protein extracts that provided a negative PCNA signal were not evaluated for COX expression.

DNA constructs and reporter plasmids

Lim and colleagues described the luciferase reporter vector (pTIS10L) that contains the promoter region of the *cox-2* gene (–963/+70 from the transcription initiation site) and the emerged 5'-deletions (–756, –547, –203, –134, –68, and –50) [25]. To examine the characteristics of potential *cox-2* cis-regulatory elements in a heterologous promoter system, oligonucleotides comprising the region of *cox-2*–66 to -38 bp were synthesized and subcloned at HindIII (5') and XhoI (3') restriction sites into the vector pT81-Luc, which contains the enhancerless herpes simplex thymidine kinase (TK) viral promoter [26] yielding construct *cox-2* (–66/–38Oligonucleotide representing the *cox-2* (–66/–38) sequence was mutated at overlapping region of CRE-Ebox element and subcloned into pT81 at Hind III (5') and XhoI (3') sites. All pT81-Luc constructs were analyzed by restriction digest and subsequently confirmed by di-deoxy sequencing. A-USF exerts its dominant-negative function by forming nonfunctional heterodimers with endogenous USF1 or USF2 proteins, inhibiting both USF1 and USF2 transactivation activities.

Transient transfections and luciferase assays

Twenty-four hours before transfection, QGP-1 cells were seeded in 5-well tissue culture plates at a density of 500 000 cells/well and grown overnight to 60% to 70% confluency. Transient transfections with 2000 ng of *cox-2*-promoter-reporter gene constructs were conducted with the Effectene transfection reagent (Qiagen, Hilden, Germany) according to the manufacturer's recommendations. To correct for transfection efficiency, each well was cotransfected with 600 ng of the Renilla luciferase vector pRL-TK (Promega, Heidelberg, Germany). To clarify the effects of transcription factors on basal *cox-2* expression cotransfection of dominant-negative USF, CREB, or USF1/2, expression constructs with appropriate *cox-2* constructs was performed as previously described [27,28]. Twenty-four hours after transfection, cells were washed with PBS and maintained for another 24 hours in serum-free Ultraculture®-medium

(Biowhittaker, Buckingham, UK) supplemented with 4 mM glutamine, 100 U/mL penicillin, and 100 µg/mL streptomycin. For the measurement of reporter gene activity, transfected cells were harvested, and luciferase activity was assayed with the Dual Luciferase Kit (Promega, Heidelberg, Germany). The luciferase activities were recorded as A.L.U. (Arbitrary Light Units) on a luminometer (Berthold-Wallac, Bad Wildbach, Germany). Results were corrected for transfection efficiency by normalizing data to Renilla luciferase activity measured in each sample. Student's *t*-test was used for the statistical analysis of the data among the groups (* $P<0.05$; ** $P<0.01$; *** $P<0.001$).

Plasmid amplification and preparation

The plasmid DNA used for the transfection experiment was extracted from transformed *Escherichia coli* cultures by the JETstar® Plasmid Maxiprep Kit (Genomed, Bad Oeynhausen, Germany). The competent *E. coli* cells (XL1-blue and AG1 strains) were transformed with isolated plasmid DNA. *E. coli* XL-1 blue was routinely used for the amplification of constructs, whereas strain AG1 was applied only for pGL3-containing constructs. Then the transformed *E. coli* were evenly spread onto an LB-plate (1% NaCl; 1% Bactotrypton; 0.5% Hefe-extract; 1.5% (w/v) Agar-Agar, pH 7.0) containing 100 µg/mL ampicillin (Boehringer, Mannheim) and cultured overnight at 37°C. A single colony was picked from the plate and seeded into 4 mL ampicillin-LB medium. After incubation at 37°C for 8 hours, the plasmid was extracted with Jetquick® Plasmid Miniprep Spin Kits (Genomed), followed by restriction enzyme digestion and electrophoresis to ensure the accuracy of the insert. Then the corresponding positive colony in the ampicillin-LB medium was preserved in 30% (v/v) glycerol at –80°C.

Electrophoretic mobility shift assays (EMSA)

Electrophoretic mobility shift assays (EMSA) analysis was used to identify nuclear proteins binding to the *cox-2* gene promoter region in GEP-NET tissues. After nuclear extracts from QCP-1 cells were prepared and cultured overnight, the medium was substituted by fresh serum-free Ultraculture® medium for 24 hours. The cells were digested with 1% trypsin/EDTA (Biochrom KG, Berlin, Germany) for 5 minutes, followed by addition of 10 mL cold PBS. The supernatant was then centrifuged and resuspended with 300 µL of Buffer A. After centrifugation, the pellet rich in cell nuclear fraction was resuspended in 40 µL of Buffer C. Nuclear protein was separated from DNA and nuclear membranes via centrifugation.

The protein level in the nuclear extract was determined by Bio-Rad method with a Protein Assay Kit® (BioRad Laboratories, Hercules, CA, USA). Nuclear extracts were quickly frozen in liquid nitrogen and stored at –80°C. After 5 µg of each complementary single-stranded oligonucleotide (Santa Cruz Biotechnology,

Santa Cruz, CA, USA) was mixed and incubated at 95°C for 5 minutes, the samples were gradually cooled. Subsequent electrophoresis determined successful annealing in 10% TBE-polyacrylamide gels.

Enzyme immunoassay (EIA) for prostaglandin E2 (PGE2) determination

To estimate COX-2 enzymatic activity, PGE2 levels were measured by enzyme immunoassay. Neuroendocrine cell lines were grown to a confluence of 90% to 100% in 6-well tissue culture plates. Cells were incubated overnight with serum-free ultra culture medium (BioWhittaker, Buckingham, UK) supplemented with 4 mM glutamine. Then 20 µM AA (final concentration of arachidonic acid in each well) was added at 15 hours and 2 hours before supernatants for determination of PGE2 was collected. In some experiments, cells were treated with the COX-2-specific inhibitor NS-398 (Cayman Chemicals, Ann Arbor, MI, USA) 10 hours before the first addition of AA until the end of the experiment. The concentration of PGE2 in cell culture supernatants was determined with a commercial EIA Kit (Cayman Chemical, Ann Arbor, MI, USA).

This assay is based on the competitive binding technique. PGE2 present in the culture supernatant of GEP-NET cell lines competes with a fixed amount of PGE2–acetylcholinesterase (AChE) conjugate (PGE2 tracer) for a limited amount of PGE2 monoclonal antibody. During the incubation at room temperature for 18 hours, this antibody-PGE2 complex binds to the goat anti-mouse polyclonal antibody that has been previously coated onto the wells of the microtiter plates. After removal of the excess conjugate and unbound sample, Ellman's Reagent (which contains the substrate to acetylcholinesterase) was added to the wells for 60 to 90 minutes to detect the bound enzyme activity. Immediately after color development, the absorbance was read at the wavelength of 412 nm. The intensity of this color, as determined by spectrophotometric detection, was proportional to the amount of PGE2 conjugate bound to the well, which is inversely proportional to the concentration of PGE2 in the sample.

Assessment of anchorage-dependent cell growth

The effects of nonselective COX-inhibitor aspirin and the COX-2-specific inhibitor NS-398 (N-[2-(cyclohexyloxy)-4-nitrophenyl]-methanesulfonamide (Cayman Chemical, USA) on anchorage-dependent cell growth of GEP-NETs were determined via proliferation assays. NS-398 was dissolved in 100% DMSO as 100 mM stock solution, whereas aspirin was dissolved in 100% ethanol as a 1 M stock solution. Different concentrations of NS-398 and aspirin were prepared freshly with cell culture medium on the day of experiments. Cells were seeded and cultured overnight in a 24-well microplate by adding 0.4 mL

of complete medium containing 5×10^3 QGP-1 cells or 1×10^4 BON cells per well. For investigating dose-response curve, the medium was replaced on day 2 and 5 by fresh growth medium in the presence of various concentrations of NS-398, corresponding solvents (DMSO for NS-398, ethanol for aspirin) or aspirin in quadruplicate. The final concentration of DMSO (0.001% to 0.2%) or ethanol (0.01% to 0.5%) in the medium did not affect proliferation. On day 8, cells in the wells were washed with PBS, harvested, and counted with an automatic cell counter COULTER Z1 (Coulter Electronics Limited, England). Staining with trypan blue revealed that ≥95% of cells were alive at the end of the experiments. To evaluate time-dependent response, cells were treated with aspirin (1 mM/well), NS-398 (20 µM/well), or corresponding solvents (DMSO for NS-398, ethanol for aspirin) for 72 hours, 96 hours, 120 hours, 144 hours, 168 hours, 192 hours, 214 hours, or 240 hours. During incubation, the reagents were changed every other day. All experiments were performed in quadruplicate cultures of identically treated cells.

Assessment of anchorage-independent cell growth (colony growth assessment)

To determine the effects of the nonselective COX inhibitor indomethacin and the specific COX-2 inhibitor NS-398 on anchorage-independent growth of GEP-NET cells, colony formation in soft agar-suspension was evaluated. Indomethacin was dissolved in 100% ethanol as 50 mM stock solution. Briefly, 3×10^4 cells were resuspended in a 1000 µL of culture medium and 300 µL of this suspension was added to a mixture of 2.7 mL of Hyclone FCS, 0.8 mL of Iscove's modified DMEM, 3.6 mL of 2.1% (w/v) methylcellulose in Iscove's, 1.6 mL agar solution (10 mL 3% agar and 20 mL DMEM) and 0.06 mL β-mercaptoethanol to obtain an agar suspension. Aliquots (1 mL, 3000 cells) of this suspension were then dispensed onto 35-mm dishes containing various concentrations of indomethacin (Sigma, Taufkirchen, Germany), NS-398 or vehicle (DMSO for NS-398, ethanol for indomethacin). Colony formation was assessed under an inverted microscope by manual counting after a 10-day incubation period. A threshold of 20 cells was arbitrarily set to score cell accumulations as colonies.

Results

Expression of the *cox-2* gene in GEP-NET tissues

Of 48 GEP-NET tissues of the foregut and midgut analyzed with COX-2 immunohistochemistry, positive COX-2 immunostaining (ranging from + to +++) was found in 84% (21 out of 25) foregut tumors and 91.3% (21 out of 23) midgut tumors. A total of 87.5% (42 out of 48) of those tissues stained positive for COX-2. Some typical patterns of COX-2 expression in these tumors are shown in Figure 1.
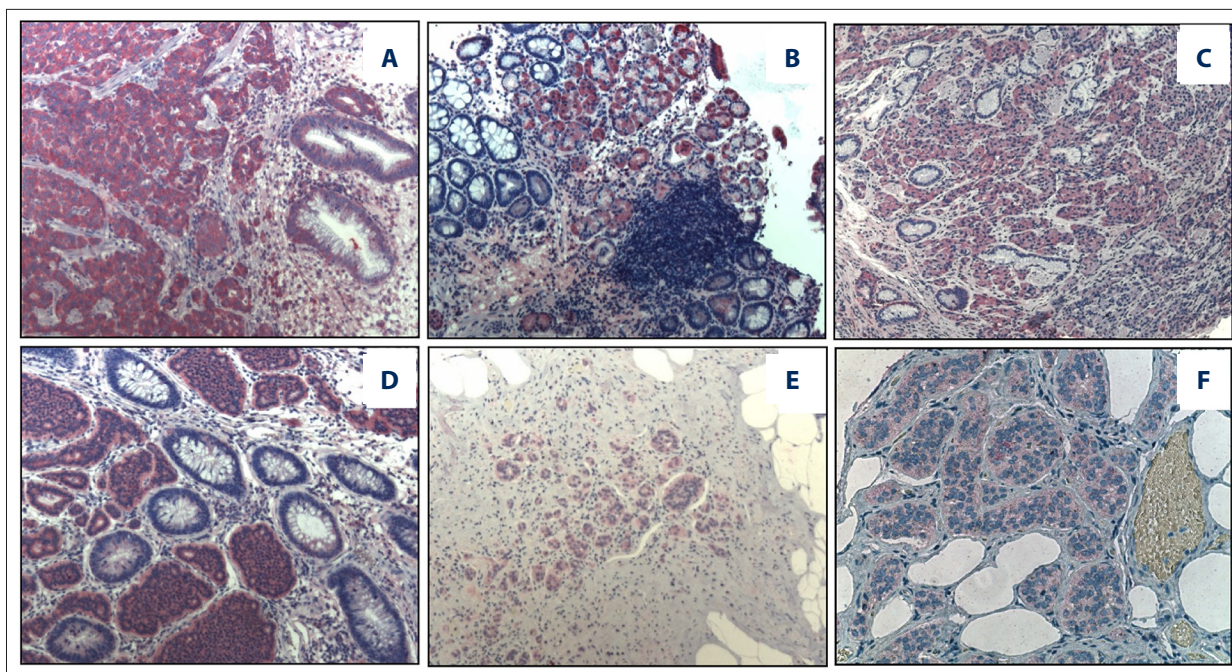
Figure 1. Immunohistochemistry in GEP-NET tissues. The COX-2-positive cells stained red. (**A, B**) gastric ECLoma; (**C**) gastrinoma of the duodenal bulb; (**D**) well-differentiated neuroendocrine carcinoma of the terminal ileum; (**E**) malignant carcinoid of the appendix with invasion of periappendical fat; (**F**) higher magnification of E. Magnification: 100× (**B, C, E**), 200× (**A, D, F**). GEP-NET – gastroenteropancreatic neuroendocrine tumors.
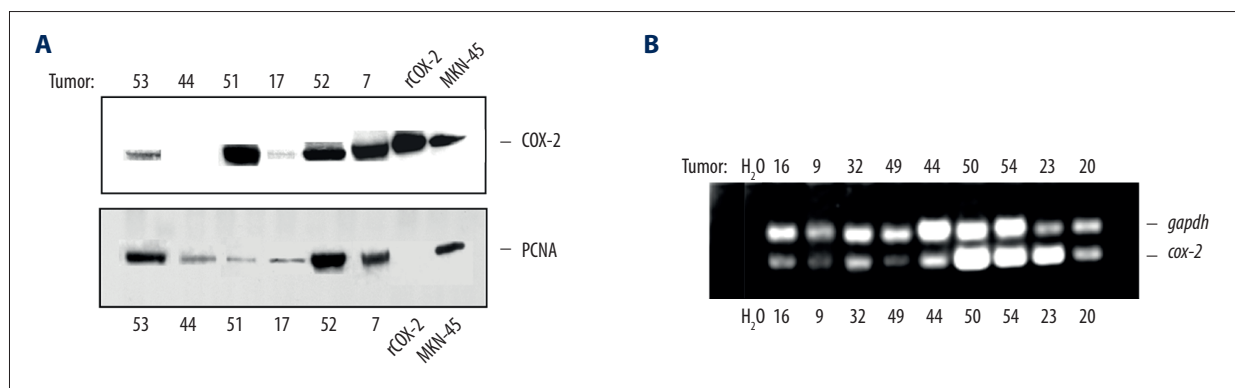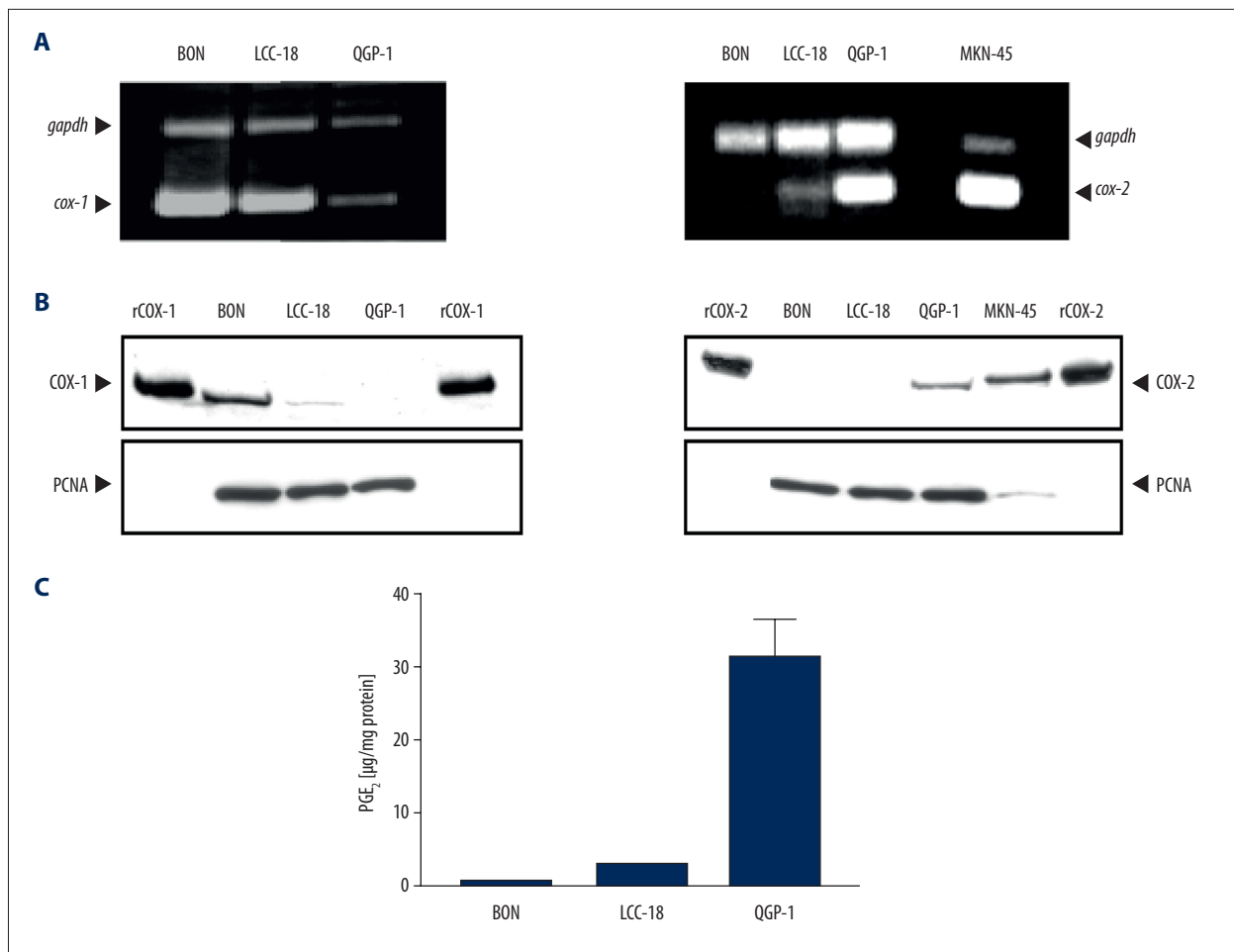

Figure 2. The analysis of *cox-2* expression by western blot and RT-PCR. COX-2 was detected by immunoblotting (**A**) using recombinant Cox-2 (lane 7) and lysates from *cox-2*-overexpressing MKN-45 gastric carcinoma cells (lane 8) as positive controls. To visualize protein loading into individual lanes, blots were stripped and reprobed with an anti-PCNA antibody. Following extraction of total RNA from GEP-NET tissue samples and reverse transcription *gapdh*-controlled duplex RT-PCR specific for *cox-2* was performed (**B**). GEP-NET – gastroenteropancreatic neuroendocrine tumors.

Positive immunoreactivity for COX-2 was demonstrated in the metastatic foci of GEP-NETs, for example, in lymph node metastasis of malignant pancreatic NET, liver metastasis of malignant ileal NET, and more strongly in venous invasion of NET.

Western blots confirmed positive results at different intensities in 5 out of 6 tumors examined for COX-2 protein. Also, *gapdh*-controlled RT-PCR confirmed *cox-2* expression in 9 out of 9 tumors. Among these 9 samples, 6 tumors were checked for

COX-2 protein by immunohistochemistry. Five tumors were positive, and 1 tumor was negative; however, RT-PCR analysis showed that these 6 tumors all expressed *cox-2* mRNA. The results from both western blot and RT-PCR are shown in Figure 2.

Figure 3. COX expression and PGE2 levels. (**A**) Duplex RT-PCR was carried out in 3 GEP-NET cell lines (BON, LCC-18 and QGP-1) with *cox-2*-overexpressing MKN-45 cells as a positive control, *gapdh* as a loading control. (**B**) Western blot analysis of COX-1/-2 expression in GEP-NET cell lines. Recombinant human COX-1 (rCOX-1) and COX-2 (rCOX-2) served as standards, protein extracts from MKN-45 gastric carcinoma cells as additional positive control, PCNA as a loading control. (**C**) PGE2 levels in the supernatants of GEP-NET cell lines. GEP-NET – gastroenteropancreatic neuroendocrine tumors.

## The *cox-1/-2* gene expression and PGE2 levels in GEP-NET cell lines

Although *cox-1* mRNA was detected in BON, LCC-18, and QGP-1 cells (left panel of Figure 3A), the COX-1 protein was detectable only in BON and LCC-18 cells (left panel of Figure 3B). Expression of *cox-2* was detectable in LCC-18 and QGP-1 cells by duplex RT-PCR (right panel of Figure 3A), whereas western blot analysis showed COX-2 protein only in QGP-1 cells (right panel of Figure 3B). Furthermore, *cox-2* mRNA expression was much higher in QGP-1 cells than LCC-18 cells with reference to the expression levels of their corresponding *gapdh* housekeeping genes (right panel of Figure 3A).

To estimate COX-2 enzymatic activity, PGE2 levels in the supernatants of GEP-NET cell lines were measured with an enzyme immunoassay. QGP-1 cells produced the highest PGE2 levels, while in LCC-18 cells and BON cells secreted the second lowest and the lowest levels, respectively (Figure 3C). This correlated very well with their expression levels of the *cox-2* gene as determined by RT-PCR. Overall, these data demonstrate that the 3 GEP-NET cell lines examined display substantial differences in *cox-2* gene expression and COX-2 enzymatic activity.

Identification of the regulatory elements and transcription factors mediating *cox-2* expression in GEP-NETs

Segments of the *cox-2* promoter region were deleted and analyzed (Figure 4A). Deletion of the promoter sequence from –963 to –68 did not affect transactivation activity, but the elimination of base pairs from –68 to –51 altered this activity, showing that these 18 base pairs are involved in *cox-2* expression in GEP-NET cells.
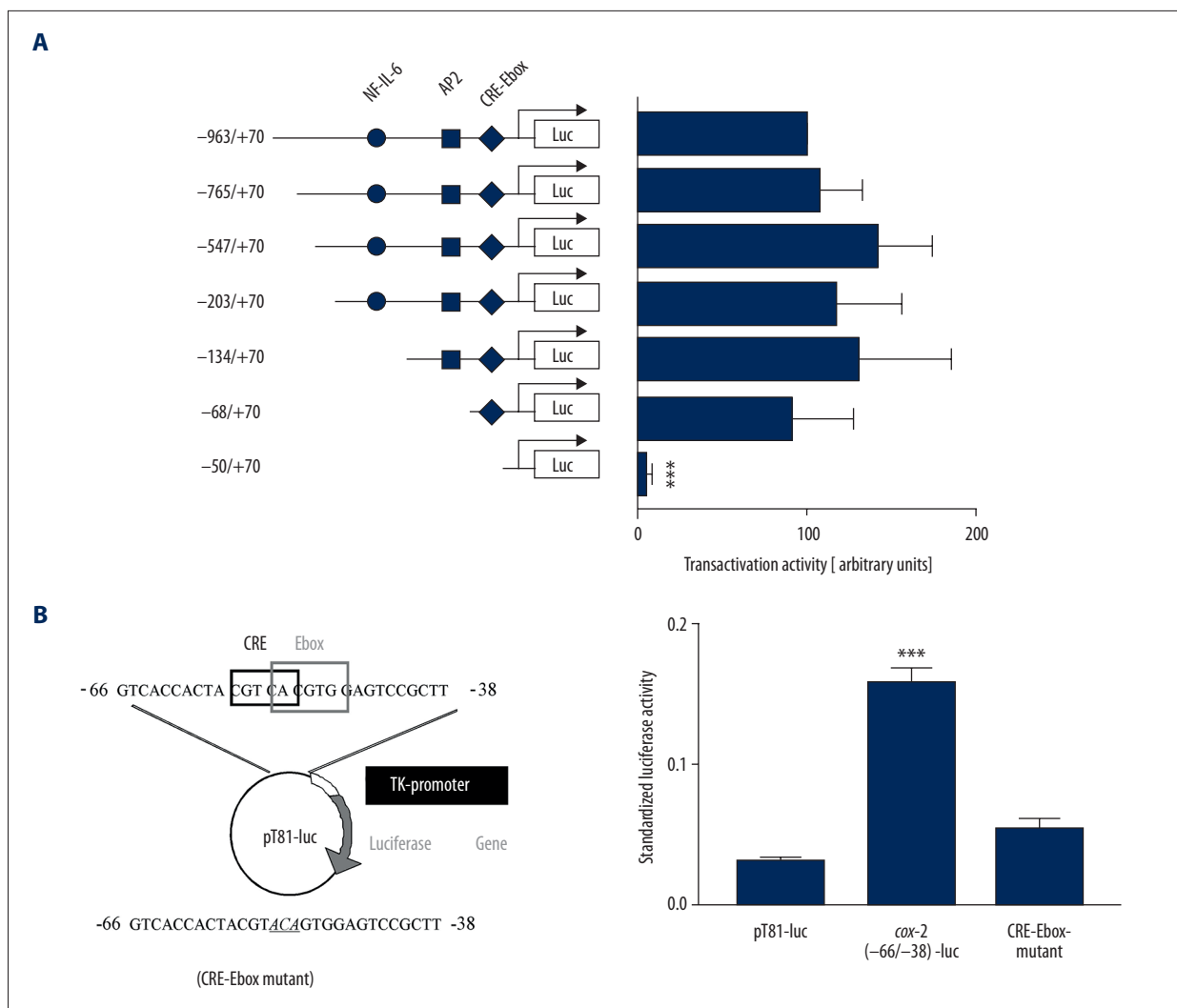
Figure 4. CRE-Ebox element & expression of the *cox-2* gene in neuroendocrine tumor cells. (**A**) The mean standardized luciferase value of construct *cox-2*-(–963/+70)-luc in each experiment was regarded as a transactivation activity of 100%. Normalized transactivation activity values of each construct were compared to that of *cox-2*-(–963/+70)-luc by Student's *t*-test for paired samples (*** *P*<0.001). (**B**) Lysates were analyzed for luciferase activities and firefly luciferase values were standardized to Renilla luciferase values. Graph shows mean standardized luciferase values (± SEM). SEM – standard error of the mean.

To further elucidate the importance of the –68/–51 region, base pairs from –66 to –38 of the *cox-2* promoter were sub-cloned into the heterologous, enhancerless pT81-luciferase vector (left panel of Figure 4B). After transfection of QGP-1 cells with this construct, the reporter gene activity increased approximately 5-fold compared with the corresponding empty vector, demonstrating that the –66/–38 element was suffi-cient to confer basal *cox-2* promoter activity (right panel of Figure 4B). The mutation of the –66/–38 sequence from CAC to ACA at the overlapping area of CRE-Ebox element (left panel of Figure 4B) resulted in complete loss of the transactivation activity (right panel of Figure 4B), suggesting that the proximal CRE-Ebox element located at *cox-2*–56/–48 is crucial for basal *cox-2* transactivation in GEP-NET cells.

Transcription factors for *cox-2* gene were also identified with EMSA analysis. Nuclear proteins were added to a specific *cox-2* sequence, the radiolabeled *cox-2*–66 to –38 (radioactive probe) and a typical probe/nuclear protein complex was formed. A mutation of this core sequence disabled the complex for-mation. The region of *cox-2* promoter sequence required for the binding of nuclear proteins and hence complex formation is the CRE-Ebox (Figure 4). The molecular identities of these transcription factors were further clarified by performing com-petition assays. The complex that was formed consisted of at least 2 different proteins that recognized different parts of the CRE-Ebox. Further EMSA analysis confirmed these results. As such, USF1/-2 and CREB transcription factors control *cox-2* pro-moter activity and gene expression in NET cells (Figures 5, 6).
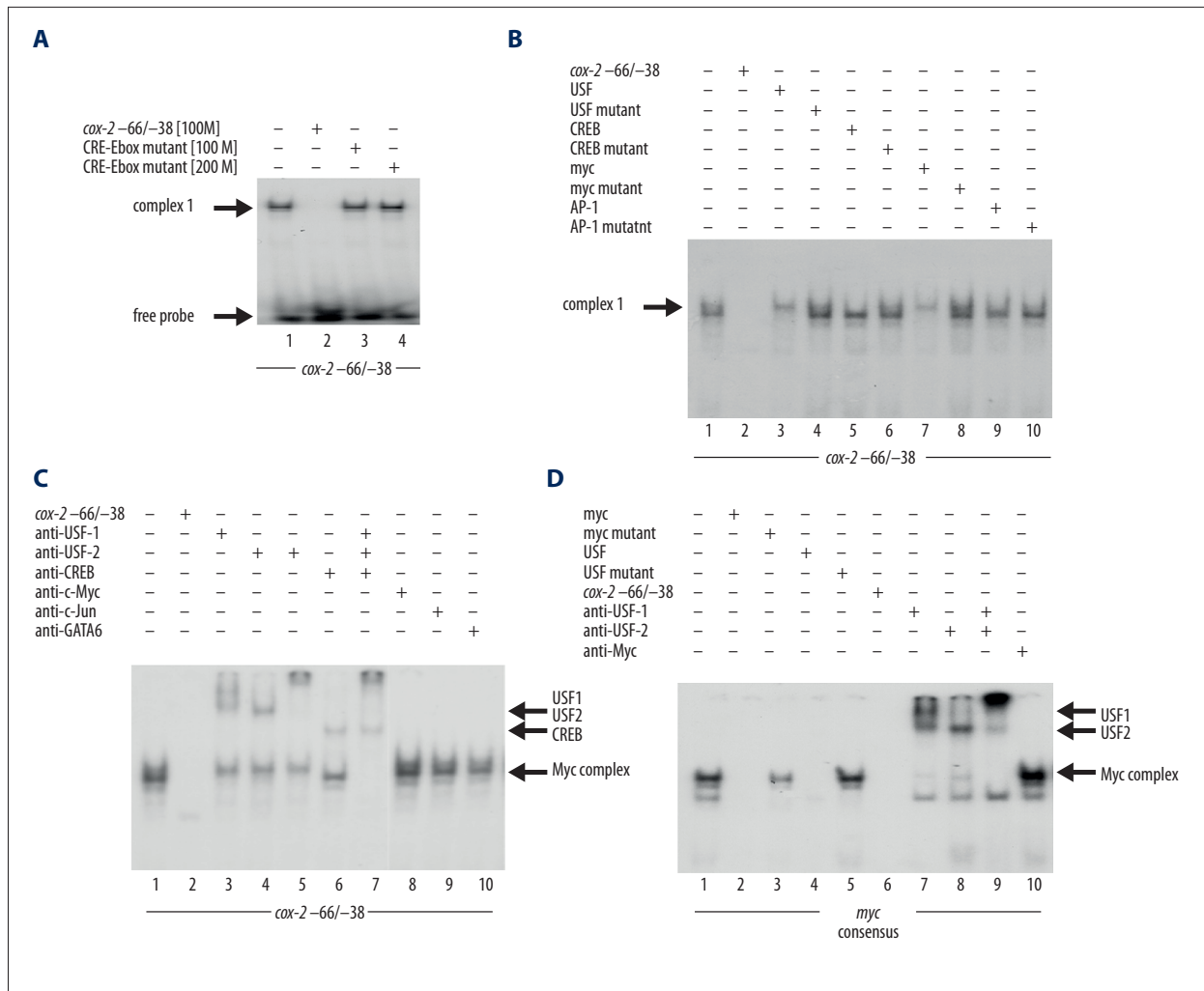
Figure 5. USF1, USF2, and CREB transcription factors bind to the proximal *cox-2* CRE/Ebox element. (**A**) *cox-2*–66/–38 probe and an excess of unlabeled nucleotides representing wild type or mutant *cox-2*–66/–38 CRE/Ebox sequences. Arrows indicate the major complex obtained with the *cox-2*–66/–38 probe (complex 1), or the localization of free, unbound radioactive probe. (**B**) Oligonucleotides are representing consensus binding sites for USF, CREB, Myc, or AP-1 transcription factor. (**C**) Arrows indicate supershifted complexes containing USF1, USF2, or CREB transcription factor. (**D**) A *myc* oligonucleotide was used as radiolabeled EMSA probe. For supershift analyses, antibodies directed against USF1, USF2 or c-Myc were applied. Arrows indicate supershifted complexes containing USF1 or USF2 transcription factors or the major complex obtained with the myc probe. EMSA – electrophoretic mobility shift assays.

Effects of NSAIDs on the anchorage-dependent growth of GEP-NET cells

To determine the COX-2-inhibitory effects of NS-398, we initially analyzed the ability of this compound to inhibit secretion of PGE2 in QGP-1 cells. The selective COX-2 inhibitor NS-398 reduced PGE2 production in QGP-1 cells in a dose-dependent manner from 1 nM to 100 nM (Figure 7E), indicating that the effective dose of NS-398 to inhibit PGE2 production was in that range. Proliferation assays were performed to determine a potential role of COX-2 in anchorage-dependent tumor cell growth. In a time-dependent response study (Figure 7A), NS-398

(20 µM/well) began to suppress QGP-1 cell growth significantly at 144 hours. The maximal inhibition rate was achieved at 240 hours. Also, NS-398 inhibited QGP-1 cell proliferation potently and dose-dependently at the dose range of 20 µM to 100 µM (Figure 7B). This dose was at least 1000-fold higher than the dose required for inhibition of PGE2 synthesis. Proliferation assays with NS-398 were also conducted in *cox-2*-negative BON cells. NS-398 was also capable of inhibiting the proliferation of BON cells dose-dependently.

To assess whether nonselective COX-2-inhibitors could also inhibit the anchorage-dependent growth of QGP-1 cells, the
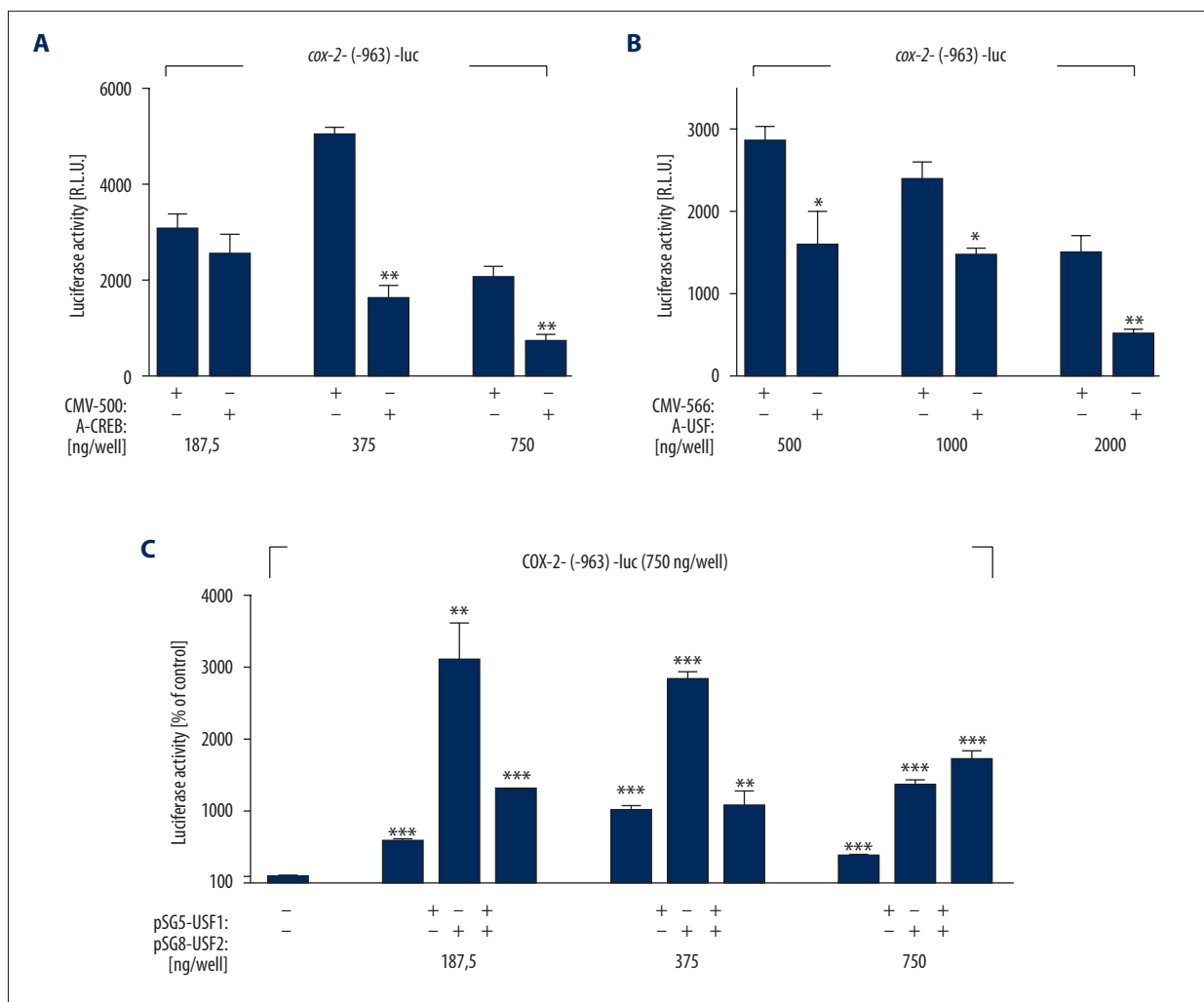
Figure 6. CREB and USF transcription factors in transactivation of the *cox-2* promoter in neuroendocrine cells. QGP-1 cells were cotransfected with indicated doses of overexpression constructs encoding for dominant-negative mutants of USF (A-USF) (**A**), CREB (A-CREB) (**B**) or pSG5-USF (**C**) along with the *cox-2*-(–963/+70)-luc reporter gene construct (750 ng/well). The graph shows the mean luciferase activity (±SEM). Luciferase values of cells transfected with A-USF, A-CREB or pSG5-USF were compared with control transfectants by using Student's *t*-test for unpaired samples (* *P*<0.05; ** *P*<0.01; *** *P*<0.001). SEM – standard error of the mean.

effect of aspirin was evaluated in proliferation assays. Similar to NS-398, aspirin (1 mM/well) started to exert the antiproliferative impact at 144 hours, and the maximal inhibition rate was achieved at 240 hours (Figure 7C). In the dose-response study, aspirin dose-dependently inhibited proliferation of QGP-1 cells (Figure 7D), with about 25% inhibition at 0.5 mM of aspirin and 100% inhibition at 5 mM of aspirin.

Effects of NSAIDs on anchorage-independent growth of GEP-NET cells

To determine the effects of NSAIDs on anchorage-independent growth of GEP-NET cells, colony formation in soft agar-suspension was evaluated in BON cells. *cox-2*-negative and

cox-2-positive BON cell lines were identified with Western blot and RT-PCR methods (Figure 8A). These cells were treated with different doses of indomethacin or NS-398. Indomethacin, which inhibits the enzymatic activity of COX-1 and COX-2 with similar specificity, dose-dependently reduced the number of colonies ranging from 0.1 to 100 μM in both *cox-2*-negative (Figure 8B) and *cox-2*-positive (Figure 8C) BON cells. NS-398 did not affect the colony formation in the dose range from 0.001 μM to 100 μM in *cox-2*-negative BON cells (Figure 8B), but it significantly and dose-dependently inhibited the number of colonies by approximately 50% in *cox-2*-positive BON cells (Figure 8C). These results suggested that in contrast to anchorage-dependent growth, selective and nonselective COX-2 inhibitors suppressed the anchorage-independent growth of GEP-NET cells
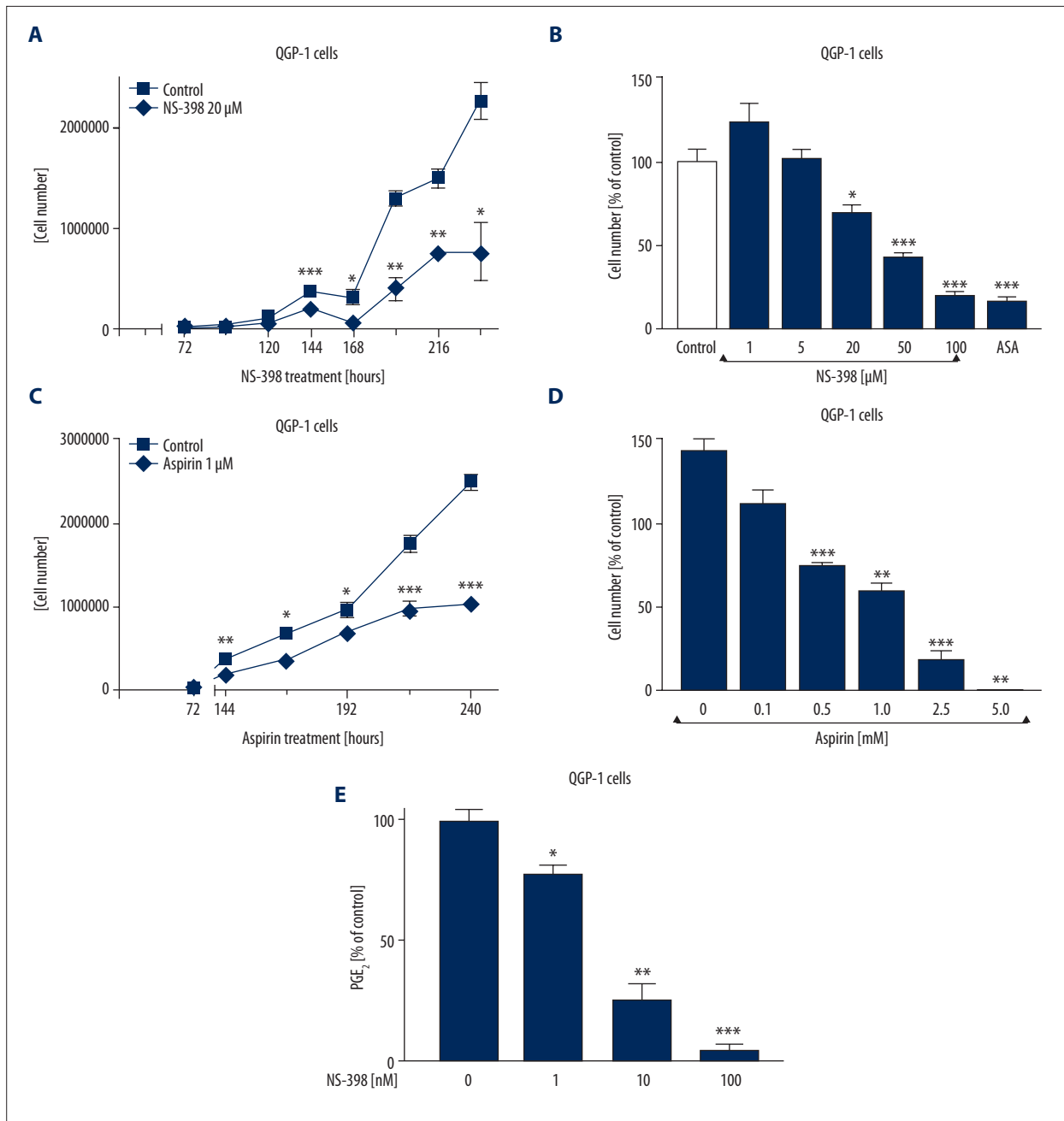
Figure 7. The inhibitory effects of selective and non-selective COX-2 inhibitors on anchorage-dependent growth in QGP-1 cell line. (**A**) The determination of the time-dependent response of NS-398. The antiproliferative effect of NS-398. (**B**) The dose-response curve of NS-398. (**C**) Time-dependent response of aspirin. (**D**) The dose-response curve of aspirin. (**E**) The inhibitory effect of the selective COX-2 inhibitor NS-398 on PGE2 production in QGP-1 cells. All the graphs show the mean normalized cell number of 4 independent experiments performed in quadruplicates, and the error bars represent the SE. Statistical significance was assessed with Student's *t*-test (* $P<0.05$; ** $P<0.01$; *** $P<0.001$ compared with the control group). SE – standard error.

through a COX-dependent mechanism. To test this hypothesis, the dose range of NS-398 for inhibiting PGE2 release was determined in *cox-2*-positive BON cells. NS-398 ranging from 1 nM to 100 nM dramatically and dose-dependently decreased

PGE2 production in *cox-2*-positive BON cells (Figure 8D), which could effectively inhibit the colony formation in this cell line (Figure 8C).
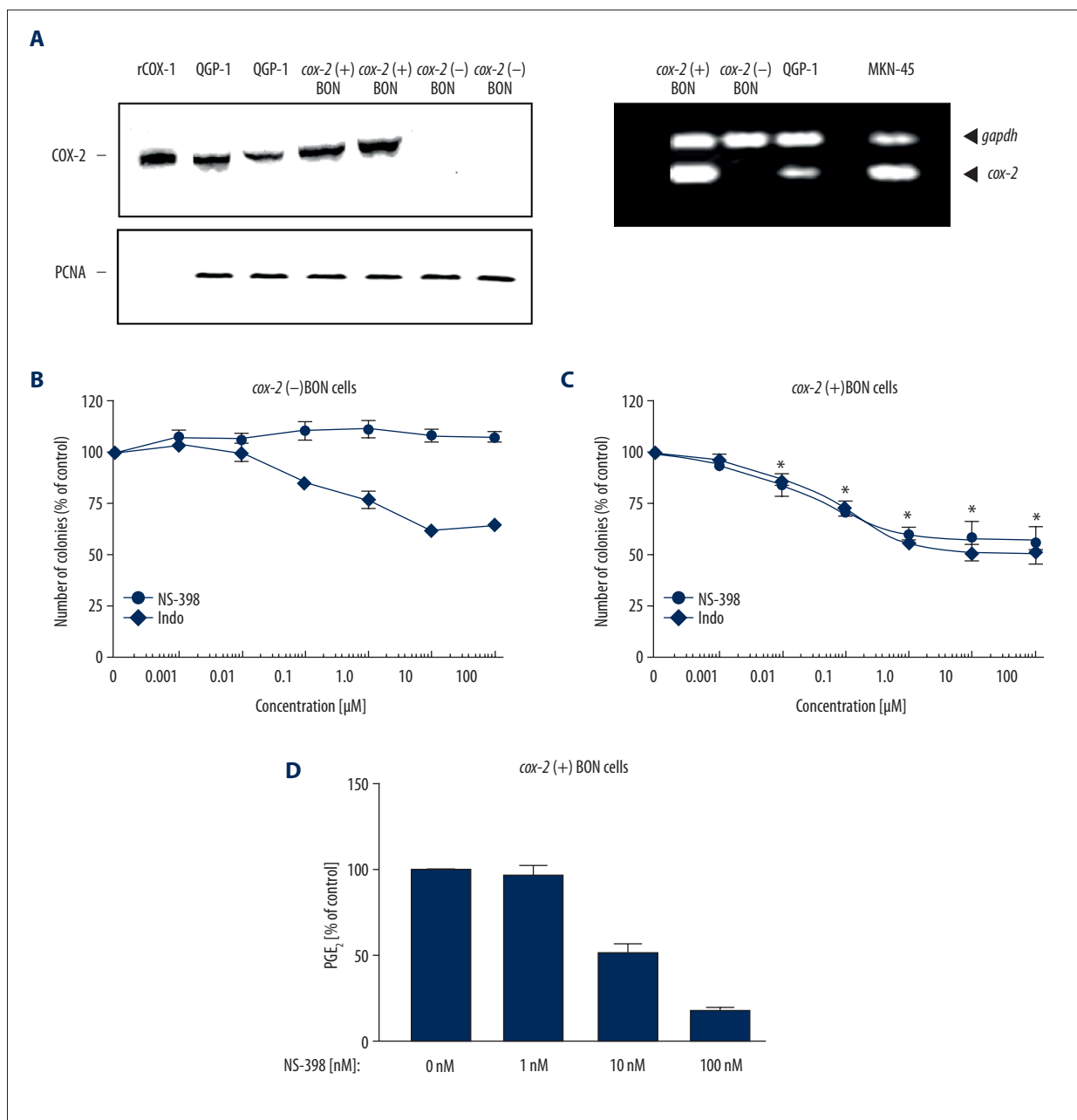
Figure 8. The selective (NS-398) and nonselective (indomethacin) COX-2 inhibitors potently suppress anchorage-independent growth of GEP-NET cells *in vitro*. This effect might be COX-dependent. (**A**) BON cells of high (*cox-2*-(+)) and low (*cox-2*-(–)) passage number were identified for *cox-2* gene expression by western-blot (left panel) or *gapdh*-controlled RT-PCR (right panel). For western blot analysis QGP-1 cell lysates as well as rCOX-2 were used as controls, while *cox-2* overexpressing MKN-45 and QGP-1 cells served as positive controls for RT-PCR. For soft agar assays *cox-2*(–) BON cells (**B**) and *cox-2*(+) BON cells (**C**) were incubated in the presence of indicated doses of NS-398 (solid circles) or indomethacin (open circles). Control cells were treated with solvents. Colony number of NS-398-treated cultures was compared with o control-cultures with the Student's *t*-test for unpaired samples (* $P<0.05$). (**D**) Also, the effect of NS-398-treatment on PGE2 secretion in *cox-2* (+) BON cells was analyzed. Graphs **B–D** show a summary of 3 independent experiments performed in triplicate.
GEP-NET – gastroenteropancreatic neuroendocrine tumors.

Discussion

COX-2 expression in GEP-NET tissues and corresponding cell lines

The current study is the first detailed analysis of *cox-2* expression in 54 pancreatic and gastrointestinal NET tissues and in 3 GEP-NET cell lines.

A total of 87.5% (42 out of 48) of GEP-NET tissues tested were positive for COX-2 expression by immunohistochemistry. Western blots confirmed positive results at different intensities in 5 of 6 tumors examined for COX-2 protein, and *gapdh*-controlled RT-PCR demonstrated *cox-2* expression at the mRNA level in 9 out of 9 tumors. The discrepancy attributed to the higher sensitivity of RT-PCR method compared with immunohistochemistry.

Further analysis of immunohistochemistry results showed that a total of 88.2% (15 out of 17) functioning tumors and 90.9% (10 out of 11) no-functioning tumors were positive for COX-2 immunoreactivity, indicating that this clinical parameter was not related to COX-2 expression in GEP-NETs. In some GEP-NETs with positive COX-2 staining in tumor cells, the staining was less intense for tumor-associated fibroblasts, inflammatory cells, and vascular endothelial cells than for tumor cells. Such positive staining of non-tumorous cells has been described in endocrine tumors previously [29,30].

Besides in primary GEP-NET tissues, COX-2 was analyzed in 3 tumor cell lines derived from such tumors. Expression of the *cox-2* gene was discovered in 2 (QGP-1, LCC-18) of 3 cell lines (Figure 3). In the third cell line (BON), COX-2-expressing and COX-2-negative clones were identified (Figure 8). Interestingly, the expression of the neuroendocrine marker molecules synaptophysin and chromogranin was apparently reduced in the *cox-2* (+) BON cells in comparison to the *cox-2* (-) BON cells, as determined by western blotting. Along with the observation that COX-2-expressing QGP-1 cells also hardly express any chromogranin or synaptophysin. This finding suggests that elevated expression of the *cox-2* gene could be a result of dedifferentiation of tumor cells. To estimate COX-2 enzymatic activity, PGE2 levels in the supernatants of GEP-NET cell lines were measured by enzyme immunoassay. QGP-1 cells produced the highest, while LCC-18 cells yielded very low and BON cells secreted the lowest PGE2. This correlated very well with their expression levels of cox-2 gene as determined by RT-PCR. These data demonstrate that the 3 GEP-NET cell lines display substantial differences in *cox-2* gene expression and COX-2 enzymatic activity.

Molecular control of *cox-2* gene expression

Expression of the *cox-2* gene is primarily controlled on a transcriptional level [31]. Several growth factors and cyto-kines including interleukin 1β (IL-1β), tumor necrosis factor α (TNF-α), platelet-derived growth factor (PDGF), estrogen, and androgen have been reported to upregulate *cox-2* gene transcription. Genomic alterations such as loss-of-function mutations of the tumor suppressor gene p53 transactivate the *cox-2* promoter [32]. There are many consensus cis-acting elements in the 5'-flanking region to regulate the transcription of the *cox-2* gene. However, analysis of regulatory promoter regions involved in transcriptional control of the *cox-2* gene revealed that only a limited number of elements including the NF-κB site, the NF-IL6 motif, and a proximal CRE-Ebox, regulate transcription independently or synergistically [33]. The present study provides a systematic analysis of the regulatory DNA elements and transcription factors controlling expression of the *cox-2* gene in GEP-NET cells.

In this study, a 5'-deletion analysis of the *cox-2* promoter was conducted in *cox-2* overexpressing QGP-1 cells. Transient transfection with 5'-deletions of the *cox-2* promoter revealed that the *cox-2* promoter could be reduced to −68/+70 of the 5' flanking sequence with retention of full transcription activity (Figure 4A), demonstrating that the main regulatory site(s) controlling *cox-2* transactivation are located at 3'-flanking region from the base pair −68. The only relevant regulatory element located in this proximal promoter region is an overlapping CRE-Ebox element [31], whereas other important regulatory elements of the *cox-2* promoter such as the NF-IL6 and NF-κB are located at 5'-flanking region of base pair −68.

To assess the relative contribution of the CRE-Ebox element to *cox-2* transactivation in GEP-NET cells, the sequence *cox-2*–66/−38 was subcloned into a heterologous promoter system (construct *cox-2*–66/−38) and a mutant thereof was constructed in which the central overlapping part of the CRE-Ebox element had been selectively mutated. This site-directed mutagenesis of the CRE-Ebox element completely abolished promoter activity (Figure 4B), indicating that the overlapping proximal CRE-Ebox sequence is a crucial element in the basal expression of *cox-2* gene. This proximal CRE-Ebox element, which is highly conserved among different mammalian species, consists of a CRE site that overlaps with an adjacent Ebox element by 2 base pairs [31,34].

After the CRE-Ebox element was identified as the central regulatory DNA element controlling *cox-2* transcription in GEP-NET cells, CREB, USF1, and USF2 were identified as transcription factors binding to this promoter element. The EMSA data strongly suggested that CREB binds to the CRE site, whereas USF1/-2 binds to the Ebox of the overlapping CRE-Ebox element. Because
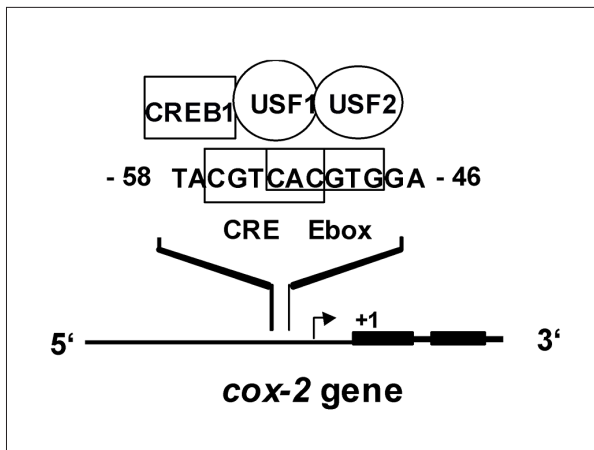
Figure 9. Sketch map of the regulatory elements and transcription factors controlling the basal expression of *cox-2* gene in GEP-NET cells. Binding of CREB and USF1/-2 to the overlapping CRE-Ebox at −56/−48 represents the core mechanism of basal *cox-2* transactivation. GEP-NET – gastroenteropancreatic neuroendocrine tumors.

both CREB and USF transcription factors contribute to *cox-2* transactivation, both the CRE and Ebox element appears to be of functional relevance for control of *cox-2* gene in GEP-NET cells. This is different from previous findings in other tumors or cells. The functional interplay of CREB and USF transcription factors that bind to an overlapping CRE-Ebox element in GEP-NET cells (Figure 9) appears to be a novel mechanism for transcriptional regulation of the *cox-2* gene in cancer cells.

The effects of NSAIDs on anchorage-dependent and -independent NET cell growth and underlying mechanisms

There is convincing evidence that NSAIDs, which inhibit cyclooxygenase activity, lower the risk of developing carcinoma of the colon, esophagus, and stomach [35]. Although the potential therapeutic efficacy of NSAIDs was related exclusively to tumors located in the digestive tract, some studies have suggested that COX-2 may be the target for the prevention and treatment of other carcinomas, including those of the prostate, breast, pancreas, head and neck, and the urinary bladder [36,37]. To date, effects of NSAIDs on GEP-NET cell lines have not been studied. Therefore, nonselective and selective COX-2 inhibitors were applied in this study to assess a potential role of COX-2 for anchorage-dependent and -independent growth of neuroendocrine tumor cells *in vitro* to ascertain whether COX-2 serves as a therapeutic target in these tumors.

The study on the effect of NSAIDs on anchorage-dependent cells shows that the proliferation of GEP-NET cells could be time- and dose-dependently inhibited by both selective (NS-398) and nonselective (aspirin) COX-2 inhibitors. Selective COX-2

inhibitor NS-398 inhibited QGP-1 cell proliferation potently and dose-dependently at the dose range of 20 μM to 100 μM. However, NS-398 reduced PGE2 production, an important end product of the enzymatic activity of COX-2, in QGP-1 cells in a dose-dependent manner from 1 nM to 100 nM. Therefore, the dose of NS-398 required for its antiproliferative action was far beyond that for its PGE2-inhibitory effect; this indicated that NS-398, a specific COX-2 inhibitor, exerted its antiproliferative effects in GEP-NET cells probably via COX-2-independent pathways. By this mechanism, NS-398 at the dose range of 50 μM to 100 μM was also capable of inhibiting the anchorage-dependent proliferation of *cox-2* (−) BON cells to a similar extent as in QGP-1 cells. To assess whether nonselective COX-2-inhibitor could also inhibit the anchorage-dependent growth of QGP-1 cells, the effect of aspirin was evaluated in proliferation assays. Similar to NS-398, aspirin (1 mM/well) started to exert the antiproliferative effect at 144 hours, and the maximal inhibition rate was achieved at 240 hours. Altogether, all these results indicate that 1) the proliferation of GEP-NET cells could be time- and dose-dependently inhibited by both selective and nonselective COX-2 inhibitors and 2) the dose-response curve for the antiproliferative effect of NS-398 shifted right relative to that for its PGE2-inhibitory action, suggesting involvement of COX-2-independent pathways in antiproliferation of this compound. Similarly, findings in *cox-2*-negative BON cells strongly support that antiproliferative effects of NS-398 are, at least to a large extent, mediated via the COX-2-independent mechanism. The exact mechanism for NSAIDs to inhibit the anchorage-dependent proliferation of GEP-NET cells needs to be further elucidated.

The study on the effects of NSAIDs on anchorage-independent growth of GEP-NET cells showed that, in contrast to anchorage-dependent growth, selective and nonselective COX-2 inhibitors suppressed anchorage-independent growth of GEP-NET cells through a COX-dependent mechanism. A nonselective COX inhibitor indomethacin and a COX-2-specific inhibitor NS-398 suppressed anchorage-independent growth of *cox-2* (+) BON cells (Figure 8C) dose-dependently. In contrast, indomethacin, but not NS-398, inhibited anchorage-independent growth of *cox-2* (−) BON cells (Figure 8B). Moreover, significant inhibition of anchorage-independent cell growth in *cox-2* (+) BON cells (Figure 8C) was observed with NS-398 doses of 10 nM to 1000 nM, which are within the range of doses required for suppression of PGE2 production in *cox-2* (+) BON cells (Figure 8D). As such, a COX-2-dependent mechanism underlies the growth inhibitory effects of NS-398 in GEP-NET cells under anchorage-independent conditions and is totally different from the COX-independent mechanism responsible for suppressing effects of NS-398 in anchorage-dependent growth of GEP-NET cells.

One limitation is that *in vitro* assays do not completely reflect *in vivo* stromal/epithelial interactions. Besides cancer cells,

stromal fibroblasts, tumor-infiltrating inflammatory cells, and angiogenic endothelial cells can express COX-2 in a tumor microenvironment [38–40]. Because either tumor cell-derived COX-2 or endothelial cell-derived COX-2 is essential in angiogenesis [41–43], COX-2 inhibitors may be effective in suppressing the growth of tumor with COX-2 expression either in tumor cells or in endothelial cells.

Conclusions

This study provides evidence that COX-2 upregulation in the majority of GEP-NETs and this upregulation may be of functional relevance in human GEP-NETs pathobiology. A functional interplay of USF1/-2 and CREB transcription factors with a proximal CRE-Ebox element is essential for *cox-2* transactivation in GEP-NET cells. This study also demonstrated that nonselective NSAIDs (aspirin and indomethacin) and selective COX-2 inhibitor (NS-398) could suppress both anchorage-dependent and -independent growth of GEP-NET cells effectively. Although the mechanisms underlying NSAIDs-mediated inhibition of anchorage-dependent GEP-NET cell growth remain unclear, the antiproliferative properties of NSAIDs may offer a novel approach to the chemoprevention and therapy of GEP-NETs.

Conflict of interests

None.

References:

1. Pape UF, Berndt U, Müller-Nordhorn J et al: Prognostic factors of long-term outcome in gastroenteropancreatic neuroendocrine tumours. Endocr Relat Cancer, 2008; 15: 1083–97

2. Montuenga LM, Guembe L, Burrell MA et al: The diffuse endocrine system: From embryogenesis to carcinogenesis. Prog Histochem Cytochem, 2003; 38: 155–272

3. Kaltsas GA, Besser GM, Grossman AB: The diagnosis and medical management of advanced neuroendocrine tumors. Endocr Rev, 2004; 25: 458–511

4. Sahani DV, Bonaffini PA, Fernández-Del Castillo C et al: Gastroenteropancreatic neuroendocrine tumors: Role of imaging in diagnosis and management. Radiology, 2013; 266: 38–61

5. Díez M, Teulé A, Salazar R: Gastroenteropancreatic neuroendocrine tumors: Diagnosis and treatment. Ann Gastroenterol, 2013; 26: 29–36

6. Metz DC, Jensen RT: Gastrointestinal neuroendocrine tumors: Pancreatic endocrine tumors. Gastroenterol, 2008; 135: 1469–92

7. Galván JA, Astudillo A, Vallina A et al: Epithelial-mesenchymal transition markers in the differential diagnosis of gastroenteropancreatic neuroendocrine tumors. Am J Clin Pathol, 2013; 140: 61–72

8. Turaga KK, Kvos LK: Recent progress in the understanding, diagnosis, and treatment of gastroenteropancreatic neuroendocrine tumors. Cancer J Clin, 2011; 61: 113–32

9. Saba NF, Choi M, Muller S et al: Role of cyclooxygenase-2 in tumor progression and survival of head and neck squamous cell carcinoma. Can Prev Res (Philla), 2009; 2: 823–29

10. Wan GX, Chen P, Yu XJ et al: Cyclooxygenase-2 polymorphisms and bladder cancer risk: A meta-analysis based on case-control studies. Int J Clin Exp Med, 2015; 8: 3935–45

11. Oshima M, Dinchuk JE, Kargman SL et al: Suppression of intestinal polyposis in Apc Δ716 knockout mice by inhibition of cyclooxygenase 2 (COX2). Cell, 1996; 87: 803–9

12. Dannenberg AJ, Altorki NK, Boyle JO et al: Cyclo-oxygenase 2: A pharmacological target for the prevention of cancer. Lancet Oncol, 2001; 2: 544–51

13. Mackenzie GG, Rasheed S, Wertheim W et al: NO-donating NSAIDs, PPARδ, and cancer: Does PPARδ contribute to colon carcinogenesis? PPAR Res, 2008; 2008: 919572

14. Ouyang N, Williams JL, Rigas B: NO-donating aspirin isomers downregulate peroxisome proliferator-activated receptor (PPAR)delta expression in APC(min/+) mice proportionally to their tumor inhibitory effect: Implications for the role of PPARdelta in carcinogenesis. Carcinogenesis, 2006; 27: 232–39

15. Gonzalez FJ, Peters JM, Shah YM: The role of peroxisome proliferator-activated receptors in carcinogenesis and chemoprevention. Nat Rev Cancer, 2012; 12: 181–95

16. Kaku M, Nishiyama T, Yagawa K et al: Establishment of a carcinoembryonic antigen-producing cell line from human pancreatic carcinoma. Gan, 1980; 71(5): 596–601

17. Funakoshi A, Tateishi K, Tsuru M et al: Pancreastatin producing cell line from human pancreatic islet cell tumor. Biochem Biophys Res Commun, 1990; 168(2): 741–46

18. Jeng YJ, Townsend CM Jr., Nagasawa S et al: Regulation of pancreastatin release from a human pancreatic carcinoid cell line *in vitro*. Endocrinology, 1991; 128(1): 220–25

19. Parekh D, Ishizuka J, Townsend CM Jr. et al: Characterization of a human pancreatic carcinoid *in vitro*: Morphology, amine and peptide storage, and secretion. Pancreas, 1994; 9(1): 83–90

20. Lundqvist M, Mark J, Funa K et al: Characterisation of a cell line (LCC-18) from a cultured human neuroendocrine-differentiated colonic carcinoma. Eur J Cancer, 1991; 27(12): 1663–68

21. Tobi M, Darmon E, Rozen P et al: Shared tumor antigens in colorectal carcinoma and neuroendocrine tumors. Cancer Detect Prev, 1998; 22(2): 147–52

22. Motoyama T, Hojo H, Watanabe H: Comparison of seven cell lines derived from human gastric carcinomas. Acta Pathol Jpn, 1986; 36(1): 65–83

23. Yokozaki H: Molecular characteristics of eight gastric cancer cell lines established in Japan. Pathol Int, 2000; 50(10): 767–77

24. Boenisch T: Education guide: Immunohistochemical staining methods: Pathology. Kumar GL, Rudbeck L, (eds.), Dako North America, Carpinteria, 5 ed., 2009; 15–20

25. Lim HY, Joo HJ, Choi JH et al: Increased expression of cyclooxygenase-2 protein in human gastric carcinoma. Clin Cancer Res, 2000; 6: 519–25

26. Murata H, Kawano S, Tsuji S: Cyclooxygenase-2 overexpression enhances lymphatic invasion and metastasis in human gastric carcinoma. Am J Gastroenterol, 1999; 94: 451–55

27. Tsuji S, Kawano S, Sawaoka H et al: Evidences for involvement of cyclooxygenase-2 in proliferation of two gastrointestinal cancer cell lines. Prostaglandins Leukot Essent Fatty Acids, 1996; 55: 179–83

28. Sawaoka H, Kawano S, Tsuji S et al: Cyclooxygenase-2 inhibitors suppress the growth of gastric cancer xenografts via induction of apoptosis in nude mice. Am J Physiol, 1998; 274: G1061–67

29. Ohike N, Morohoshi T: Immunohistochemical analysis of cyclooxygenase (COX)-2 expression in pancreatic endocrine tumors: Association with tumor progression and proliferation. Pathol Int, 2001; 51: 770–77

30. Cadden IS, Atkinson AB, Johnston BT et al: Cyclooxygenase-2 expression correlates with phaeochromocytoma malignancy: Evidence for a Bcl-2-dependent mechanism. Histopathology, 2007; 51: 743–51

31. Molina MA, Sitja-Arnau M, Lemoine MG et al: Increased cyclooxygenase-2 expression in human pancreatic carcinomas and cell lines: Growth inhibition by nonsteroidal anti-inflammatory drugs. Cancer Res, 1999; 59: 4356–62

32. Smith WL, DeWitt DL, Garavito RM: Cyclooxygenases: Structural, cellular, and molecular biology. Annu Rev Biochem, 2000; 69: 145–82

33. Gaulart Filho JA, Nonaka CF, Miguel MC et al: Immunoexpression of cyclooxygenase-2 and p53 in oral squamous cell carcinoma. Am J Otolaryngol, 2009; 30: 89–94

34. Tanabe T, Tohnai N: Cyclooxygenase isozymes and their gene structures and expression. Prostaglandins Other Lipid Mediat, 2002; 68–69: 95–114

35. Rao CV, Reddy BS: NSAIDs and chemoprevention. Curr Cancer Drug Targets, 2004; 4: 29–42

36. Sobolewski C, Cerella C, Dicato M et al: The role of cyclooxygenase-2 in cell proliferation and cell death in human malignancies. In J Cell Biol, 2010; 2010: 215158

37. Greenhough A, Smartt HJ, Moore AE et al: The COX2/PGE2 pathway: Key roles in the hallmarks of cancer and adaptation to the tumour microenvironment. Carcinogenesis, 2009; 30: 377–78

38. Kitadai Y: Cancer-stromal cell interaction and tumor angiogenesis in gastric cancer. Cancer Microenviron, 2010; 3: 106–16

39. Tjomsland V, Niklasson L, Sandström P et al: The desmoplastic stroma plays an essential role in the accumulation and modulation of infiltrated immune cells in pancreatic adenocarcinoma. Clin Dev Immunol, 2011; 2011: 212810

40. Rüegg C, Dormond O, Mariotti A: Endothelial cell integrins and COX2: Mediators and therapeutic targets of tumor angiogenesis. Biochim Biophys Acta, 2004; 1654: 51–67

41. Brown JR: Cyclooxygenase as a target in lung cancer. Clin Cancer Res, 2004; 10(12 Pt 2), 4266s–69s

42. Klenke FM, Gebhard M, Ewerbeck V et al: The selective Cox2 inhibitor celecoxib suppresses angiogenesis and growth of secondary bone tumors: An intravital microscopy study in mice. BMC Cancer, 2006; 6: 9

43. Dettmeyer R: Forensic histopathology: Fundamentals and perspectives. Dettmeyer R (ed.), Springer, Berlin Heidelberg, 2011; 17–35